Physica B xxx (xxxx) xxx–xxx

Contents lists available at ScienceDirect

Physica B

journal homepage: www.elsevier.com/locate/physb

Kondo temperature and Heavy Fermion behavior in $Yb_{1-x}Y_xCuAl$ series of alloys

D.P. Rojas[a,*], F.G. Gandra[b], A.N. Medina[c], L. Fernández Barquín[d], J.C. Gómez Sal[d]

[a] Dpto Estructuras y Física, ETSAM, Universidad Politécnica de Madrid, Madrid, Spain
[b] Instituto de Física, Universidade Estadual de Campinas, Campinas, Sao Paulo, Brazil
[c] Dpto Física, Universidade Estadual de Maringa, Maringá, Paraná, Brazil
[d] Dpto CITIMAC, Facultad de Ciencias, Universidad de Cantabria, Santander, Spain

ARTICLE INFO

Keywords:
Yb alloys
Intermediate valence
Heavy fermion
Kondo temperature
Electrical resistivity
Specific heat

ABSTRACT

Results on x-ray diffraction, electrical resistivity, specific heat and magnetization on the $Yb_{1-x}Y_xCuAl$ series of compounds are reported. The analysis of the x-ray data shows the increase of the unit cell volume with the Y dilution. The electrical resistivity shows an evolution from Kondo lattice regime for $x \leq 0.6$ to single impurity behavior for $x = 0.8$ and 0.94. The electronic coefficient γ shows values of Heavy Fermion systems along the series for $0 \leq x < 1$. On the other hand, dc magnetic susceptibility measurements show typical curves of intermediate valence systems with a maximum around 25 K. Below this maximum, the values of low temperature susceptibility ($\chi(0)$) decrease with the increase of Y content. From the dependence of $\chi(0)$ and γ upon Y substitution, an increase of 12% of the Kondo temperature (T_K) for $x = 0.8$ alloy respect to the reference YbCuAl ($x = 0$) is estimated. This is further supported by the evolution of the temperature of the maximum in the magnetic contribution of the specific heat. The overall results can be explained by the increase of the hybridization as consequence of *negative pressure effects* obtained by the chemical substitution of Yb by Y, thus leading to the increase of T_K, in agreement with the Doniach's diagram.

1. Introduction

Nowadays, Yb - based alloys still continue being a subject of extensive studies within the Strongly Correlated Electron Materials area of research because the variety of ground states they present [1]. Most of the Yb compounds are found in the non-magnetic ground state, and the tune of their interesting properties has been mainly carried out by hydrostatic pressure experiments, in which both Jn_f parameter (J is the coupling constant between $4f$ and conductions electrons, and n_f is the density of states at the Fermi level) and the Kondo temperature ($T_K \propto exp(-1/Jn_f)$) are expected to decrease when increasing pressure [2]. This kind of studies appears to be of great interest in disclosing novel phenomena because the systems move towards the magnetic instability or to the Quantum Critical Point (QCP), when coming from the non-magnetic state [3]. Alternatively, less attention has been paid to experimental evidences of *negative pressure effects*, in the right-hand side of the peak in Doniach's magnetic phase diagram [4,5], when the systems move away from the QCP. It is then worthwhile to explore the region of higher hybridization states, when some theoretical and experimental reports point even, to the existence of anomalous Kondo behaviors [6,7]. Among the Yb systems, the archetypal intermediate valence and *Heavy Fermion* YbCuAl alloy has been a subject of several studies [8–15]. YbCuAl alloy is characterized as intermediate valence material with a high value of $T_K = 66$ K [2]. This kind of system presents a characteristic temperature above which a local description of the $4f$ electrons seems applicable, but below this temperature the Fermi liquid picture is more adequate. For YbCuAl this occurs between 20 and 30 K. Moreover, electrical resistivity measurements under pressure up to 8 GPa showed that T_K is reduced almost 8 times [14]. The studies on the $Yb_{1-x}Sc_xCuAl$ series of alloys showed an increase of both low temperature magnetic susceptibility values $\chi(0)$ and electronic coefficient (γ) [12] with the Sc substitution (decrease of the unit cell volume), which point towards a reduction of T_K [2], in agreement with the hydrostatic pressure experiments. The same tendency was found from specific heat measurements under pressure up to 10 kbar showing an increase of 30% of γ [10]. This reduction of T_K upon application of pressure is observed in many Yb compounds and it is associated to a reduction of J due to the induced volume contraction [16]. This trend is in fact the opposite to the behavior found in Ce compounds. On the other hand, $Yb_{1-x}Y_xCuAl$ series of alloys have shown the expansion of the unit cell volume with the increase of the Y content [8], suitable for the study of *negative pressure* effects on the physical properties of

* Corresponding author.
E-mail address: d.rojas@upm.es (D.P. Rojas).

http://dx.doi.org/10.1016/j.physb.2017.09.096
Received 27 June 2017; Received in revised form 18 September 2017; Accepted 22 September 2017

pristine YbCuAl alloy. In this work, a more complete characterization of the $Yb_{1-x}Y_xCuAl$ series of alloys is provided including the analysis of the thermal and electronic transport properties, giving a further inside on the T_K and *Heavy Fermion* behavior.

2. Experimental

The samples of the $Yb_{1-x}Y_xCuAl$ series of alloys were prepared using an arc-furnace and high purity materials: Yb (99.9%), Y (4 N), Cu (5 N) and Al (5 N) (All from Alfa-Johnson Matthey). They were melted with excess of Yb (15–20%) to compensate for losses during the fusion. Afterwards an annealing at 700 °C for one week was performed. X-ray diffraction patterns of the samples were recorded at 300 K in a Philips PW1710 diffractometer using CuK_α radiation and a graphite secondary monocromator.

Dc-magnetic susceptibility measurements were carried out in a Quantum Design MPMS (Magnetic Properties Measurement System)-SQUID magnetometer device in the temperature range between 2 K and 300 K at the magnetic field of 1 kOe. The curves were recorded on warming in a FC (Field Cooling) regime, with measuring steps of 0.2 K and 0.5 K in the low temperature region below 30 K, and of 1 –2 K at higher temperatures. Here, the masses of samples were around 30 mg.

The electrical resistivity was measured using a standard four-probe dc method in a temperature range between 1.5 k and 300 K. The samples used in these measurements were in the form of sheets with thickness of 1– 2 mm, width 2–4 mm and length 4–6 mm, previously cut in a diamond saw. The contacts were assured by gold wires under mechanical pressure. The curves were recorded in a sweep mode (1–2 K/min) on warming, and with different steps of temperature between 0.05 K and 1 K. The current applied during the experiments was 4–20 mA, with a stability of 0.001 mA, and the voltage was controlled by a Keithley nanovoltmeter (Model 182). A full description and more details of the set up can be found elsewhere [17].

The specific heat (c_p) was measured in a small sample calorimeter [18,19], using the thermal relaxation method between 5 K and 80 K. The experimental setup involves a sample which is attached to a sample platform with a thermal grease. The platform consists of a thin sapphire sheet, which has high thermal conductivity. In all measurements, the grease was placed on the sample platform and weighed. The contribution of the grease, was measured over the temperature range 5–80 K before the sample (mass 10–20 mg) was loaded onto the platform. Then the grease contribution is subtracted from the total measured heat capacity (with the mounted sample) to obtain the intrinsic specific heat of the sample. The system has a 5% accuracy in the temperature range of the measurements [18,19], which is similar to that reported for current commercial equipments [20].

3. Results

3.1. Structural characterization

The analysis of x-ray diffraction patterns shows that the reflections can be identified as coming from the space group *P-62m*, as shown in Fig. 1, as an example, for the intermediate concentration $x = 0.6$ with lattice parameters $a = 6.995(8)$ Å, and $c = 4.028(7)$ Å. Both a and c lattice parameters vary linearly according to Vegard's law with the Y concentration (x), from those of the YbCuAl ($a = 6.931(4)$ Å, $c = 3.992(3)$ Å), to YCuAl ($a = 7.051(3)$ Å, c = 4.045(4) Å). Consequently, the same occurs with the unit cell volume along the series (see right inset of Fig. 1), as already observed in other studies on the same system [8]. Additionally, the samples crystallize with the ZrNiAl (Fe_2 **P**) type of structure formed by a plane of Yb and Al atoms between two others of Cu and Al atoms, as shown in the left inset of Fig. 1.

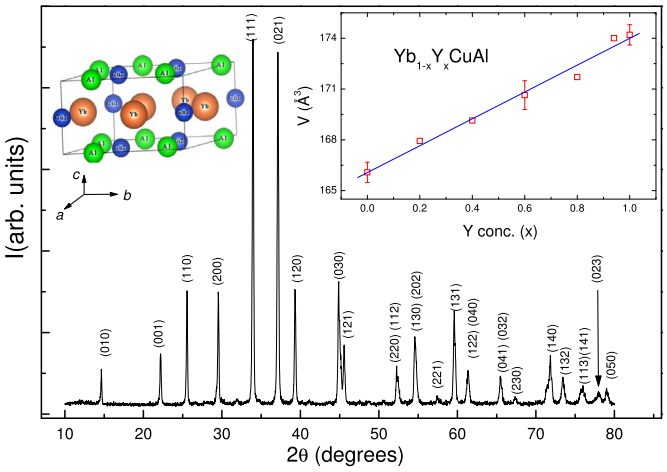

Fig. 1. x-ray diffraction pattern of $Yb_{0.4}Y_{0.6}CuAl$ alloy with the indexed positions according to the ZrNiAl (*P-62 m*) type of structure. Right inset: unit cell volume dependence with the Y concentration (x) along the series, according to the analysis of the x-ray diffraction data. A linear dependence of both the unit cell parameters and volume is obtained. Left inset: Crystallographic structure of the pristine YbCuAl alloy with the distributions of the different atoms.

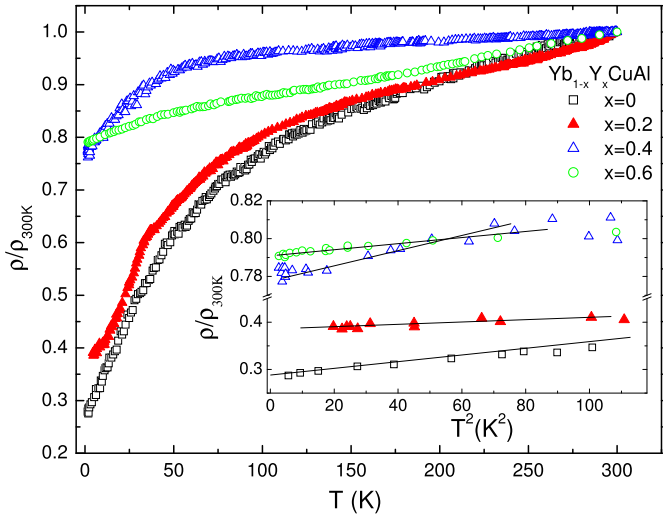

Fig. 2. Temperature dependence of the electrical resistivity for several Yb concentrations within the Kondo lattice regime. The inset details the low temperature region with the AT2 dependence characteristic of the Fermi liquid behavior. The solid lines are just guides to the eyes.

3.2. Electrical resistivity

The electrical resistivity vs temperature curves normalized at 300 K for Y concentrations $0 \leq x \leq 0.6$ are presented in Fig. 2. The samples show a decrease of the resistivity at low temperatures, which is a characteristic of the *Kondo lattice* systems. The inset shows the low temperature region ($T < 10$ K) showing a $A\ T^2$ dependence, as a distinctive feature of the Fermi liquid behavior. The analysis of the data indicates a decrease of the A parameter with the Y dilution (or decrease of the Yb concentration), as listed in Table 1. For Y concentrations $0.8 \leq x < 1$, a deviation from the Fermi liquid behavior is observed, with the increase of the electrical resistivity on going to lower temperatures (Fig. 3), and with the presence of a minimum at 20 K and 30 K, for $x = 0.94$ and 0.8, respectively, as depicted in the inset. The $x = 1$ (YCuAl) compound presents a metallic behavior which is described by the Bloch–Grunëisen law [21] with parameters $\theta_D = 286\ K$ (Debye temperature), $R = 0.135\ \mu\Omega$ cmK^{-1} (electron phonon interaction constant) and $\rho_0 = 32\ \mu\Omega$cm (residual resistivity), as indicated by the solid line. The magnetic contribution to the electrical

Table 1
Values of the A coefficient in the AT^2 dependence of the electrical resistivity in the low temperature region (T < 10 K).

Series	conc.(x)	A ($\mu\Omega$cmK^{-2})
$Yb_{1-x}Y_xCuAl$	0	0.05267
	0.2	0.04630
	0.4	0.02690
	0.6	0.01386

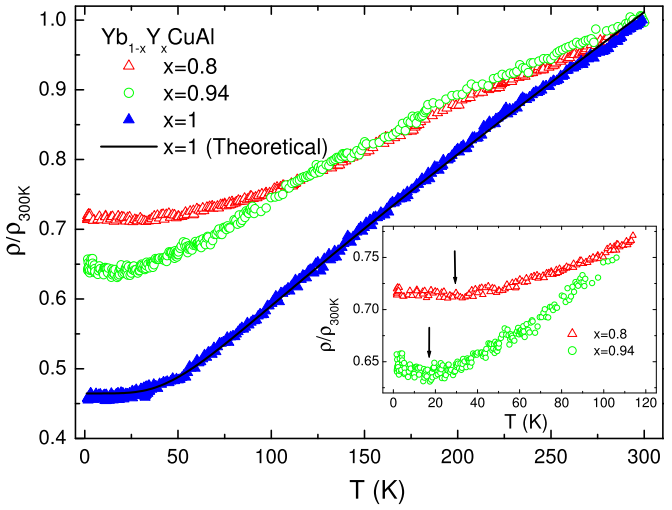

Fig. 3. Temperature dependence of the electrical resistivity curves for low Yb concentrations, showing the transition to a single impurity regime. For x = 1 (YCuAl) a metallic behavior according to the Bloch-Grüneisen law is observed. The inset details the region of temperatures where a minimum is observed.

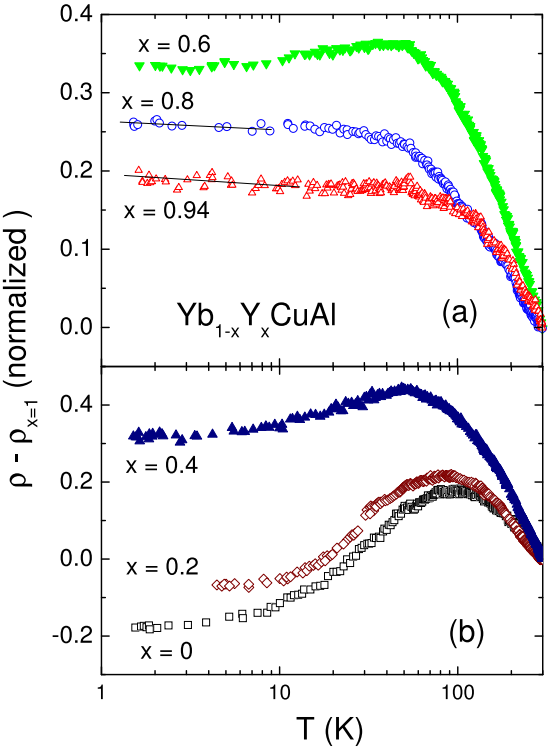

Fig. 4. Magnetic contribution to the electrical resistivity for $Yb_{1-x}Y_xCuAl$ series of alloys, normalized at 300 K. a) For low Yb concentrations, a crossover between Kondo lattice and single impurity regimes, and the -lnT dependence at low temperatures for x = 0.8 and 0.94 are observed. b) Yb concentrations within the Kondo lattice regime with a high temperature -lnT dependence, and a resistivity drop below the maximum.

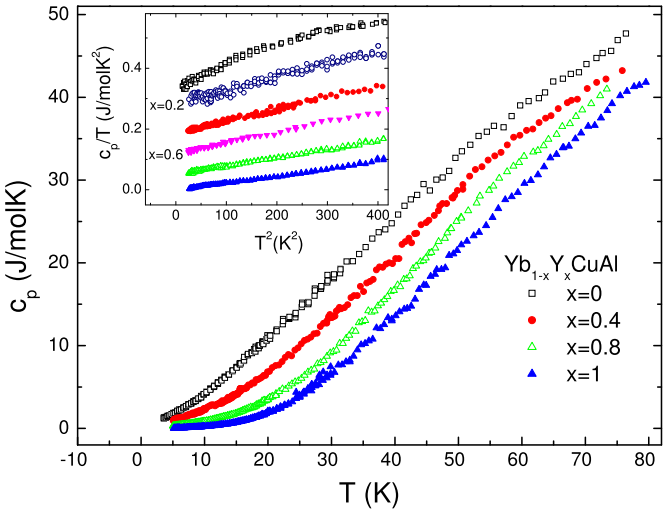

Fig. 5. Specific heat vs. temperature curves for $Yb_{1-x}Y_xCuAl$ series of alloys. The inset displays the c_p/T vs T^2 dependence indicating a change in the electronic coefficient gamma (γ) along the series.

resistivity can be estimated by subtracting the reference YCuAl (x = 1) and the results are depicted in Fig. 4. For $0 \le x \le 0.6$ we observe the presence of the incoherent Kondo scattering above the maximum, for T > 100 K, and the onset of coherence of the *Kondo lattice* at lower temperatures below 50 K, as reported for YbCuAl [11]. A different behavior is found for low Yb concentrations for x = 0.8 and x = 0.94. Here the maximum is not well defined, and there are two regions of the incoherent Kondo scattering, with the -lnT dependence. Thus, a change in the low temperature regime is observed for concentrations around x = 0.7.

3.3. Specific heat

The specific heat vs. temperature curves up to 80 K for several concentrations is shown in Fig. 5. For the sake of clarity the experimental data for x = 0.94 is not shown because it is very close to that of x = 1. The inset details the low temperature region of c_p/T vs T^2 curves, with a linear behavior according to the contribution of electrons and phonons [21]. The fitting of the curves for T < 20 K provides the values of the electronic coefficient (γ) along the series, thanks to the extrapolation of the curves c_p/T to T⟶0, and the results are collected in Table 2. For x = 1, the value is according to that expected for normal metals [22], whereas for the rest of concentrations the values are characteristic of moderate *Heavy Fermion* systems, with decreasing values with the Y dilution. According to the Bethe-ansatz solution of the Coqblin-Schrieffer model [23,24], γ scales with the characteristic temperature T_K following the proportionality $\gamma \sim 1/T_K$. Thus, according to this relation and the values of γ extracted from the specific heat data, it is expected an increase of T_K with the Y concentration (x). In order to check this possibility, the magnetic contribution to the specific heat (c_{mag}) is estimated up to x = 0.8 by subtracting the reference YCuAl (x =

Table 2
Values of the electronic coefficient (γ), as obtained from the analysis of the specific heat data.

Series	conc.(x)	γ(mJ/molK^2)	γ(mJ/molYbK^2)(±3%)
$Yb_{1-x}Y_xCuAl$	0	340	340
	0.2	268	335
	0.4	188	313
	0.6	120	300
	0.8	50	250
	0.94	11	183
	1.0	5.5	–

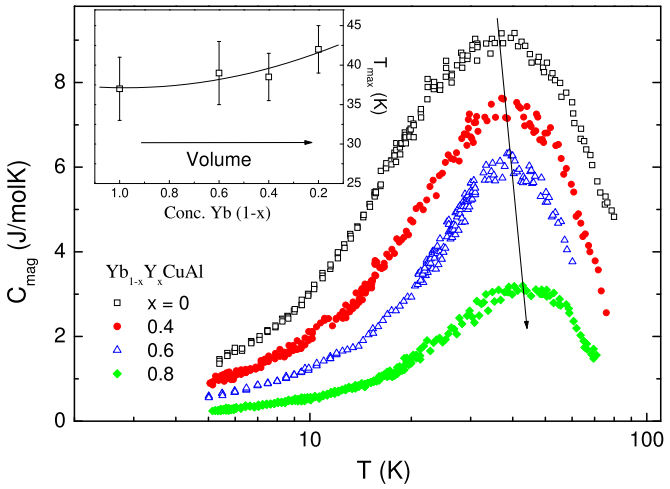

Fig. 6. Magnetic contribution to the specific heat for $Yb_{1-x}Y_xCuAl$ series of alloys estimated by subtracting the reference YCuAl (x = 1) alloy. The inset shows the evolution of the maximum with the Yb concentration (or Y-dilution process).

1) alloy. We are here considering that the phonon contribution is the same for all samples of the series. The results are presented in Fig. 6. The appearance of a maximum in c_{mag} for YbCuAl has been associated to the Kondo contribution to the specific heat, described by the $J = 7/2$ Coqblin-Schrieffer model with the value of $T_K = 66$ K [2,25]. The inset shows the dependence of the temperature of the maximum (T_{max}), on the Yb concentration (or increase of the Y content), where the arrow indicates the direction of unit cell volume increase. Taking $T_{max} \propto T_K$ [2], then, this last result suggests an increase of T_K with the unit cell volume, in agreement with the γ behavior.

3.4. dc magnetic susceptibility

The temperature dependence of magnetic susceptibility $\chi = M/H$ for several samples is shown in Fig. 7. All the curves display a Curie-Weiss paramagnetic contribution for temperatures above the maximum (around 25 K), with an effective magnetic moment near to that expected for the free Yb^{3+} ($\mu_{eff} = 4.54\mu_B$). Below the maximum, there is an increase for all samples on going to lower temperatures. The presence of this upturn commonly found in intermediate valence Yb compounds is associated to the existence of trivalent Yb^{3+} impurities

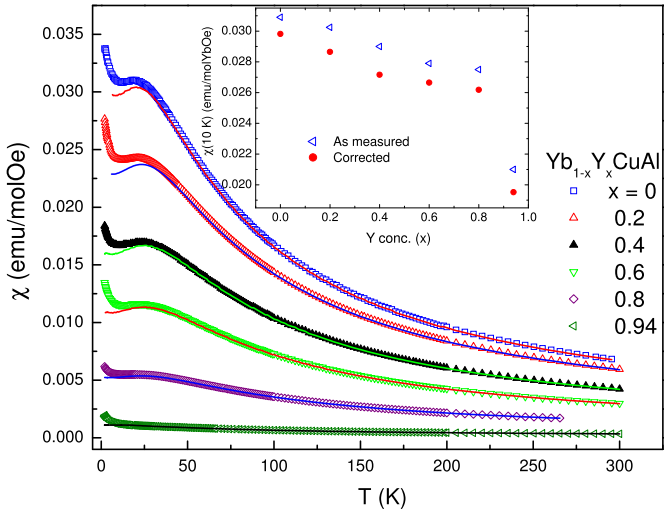

Fig. 7. DC magnetic susceptibility ($\chi = M/H$) vs. temperature curves for $Yb_{1-x}Y_xCuAl$ series of alloys under applied magnetic field of 1 kOe. The solid lines are the correction for Yb^{3+} impurities. The inset details the estimate of the low temperature values ($\chi(0)$) in the Pauli regime, below the maximum.

[8,13,26]. The procedure of correction of the contribution of this impurities we have used is similar to that performed in the study of intermediate valence $YbAl_3$ material, with the use of the experimental data of reference Yb_2O_3 oxide and by fitting of low temperature region (T < 12 K) with a modified Curie-Weiss law [26]. The solid lines in Fig. 7 represent the M/H vs T dependence after corrections for such impurities, being around of 0.6% in our samples. Now, at lower temperatures a near constant value is observed, in agreement with the expected Pauli regime (Fermi Liquid behavior) [2,3,24]. The inset shows the dependence of low temperatures values $\chi(0)$ as measured and after corrections taken at 10 K (showing the same tendency and relative variation) as a function of the Y concentration (x). The values of $\chi(0)$ (as measured) for $x = 0$–0.8 are around 10% higher and 15% lower ($x = 0.94$), respect to those already observed in other studies of this series of alloys [8,13]. This difference could arise due to different procedures of preparation of the samples which may lead to small deviations from nominal composition within a solubility range $Yb(Cu_{0.55\text{-}0.50}Al_{0.45\text{–}0.50})_2$ [27]. This fact has been already observed in measurements of the magnetic properties of YbCuAl samples annealed at different temperatures of 700 °C and 760 °C [11]. Our analysis of the x-ray diffraction data of YbCuAl gives the lattice parameters (a = 6.931(4) Å, c = 3.992(3) Å), which are close to those observed for the nominal composition $Yb(Cu_{0.50}Al_{0.50})_2$ [27]. Consequently, it is clear that the effects of Y alloying on the physical properties of starting alloy are valid. The last comment is addressed to $x = 0.94$ sample, where the maximum is hardly observed, even after corrections, and the low temperatures values deviates from the tendency of the rest of samples (see inset of Fig. 7). This fact will be commented in the discussion topic when comparing γ and T_K values.

Following the results of the solution of the Coqblin-Schrieffer model, the zero-temperature susceptibility $\chi(0) \propto 1/T_K$ [2,23]. Thus, similar to that obtained from the analysis of specific heat data, a tendency of increase of T_K with the chemical substitution of Yb by Y is also obtained from the $\chi(0)$ values of dc magnetic susceptibility results. Regarding the evaluation of the T_K behavior, it is adequate to count not only with the dc magnetic susceptibility results but also with the electrical resistivity and specific heat measurements. This is the complete procedure developed here. Hence, the results become fully supported.

4. Discussion

From the electrical resistivity results for samples of the $Yb_{1-x}Y_xCuAl$ series of alloys, a change of regime at low temperatures from *Kondo Lattice* ($0 \leq x \leq 0.4$) to single impurity (-lnT) for $x = 0.8$ and 0.94 is observed. In fact, it is found that the periodicity of the array of magnetic ions [4,5] is broken by the chemical substitution by the non-magnetic Y around $x = 0.7$. For samples with $x \leq 0.6$ the Fermi liquid dependence AT^2 at low temperatures, is observed. The values of A coefficient decreases with the increase of the Y content, as given in Table 1. It is well known that the *Kadowaki-Woods* relation is followed by a large number of *Heavy Fermion* systems $A/\gamma^2 = 10^{-5}\ \mu\Omega\ \text{cm}\cdot mol^2\ \text{K}^2\ \text{mJ}^{-2}$. However, a deviation from this relation has been observed for Yb systems with almost fully degenerated $J = 7/2$ ground state. In Fig. 8(a) the A vs γ^2 values are plotted (in log-log scale) for several concentrations between $x = 0$ and $x = 0.6$. It is found that the values follow the relation $A/\gamma^2 = 1.4 \times 10^{-6}\mu\Omega\text{cm}\cdot mol^2\text{K}^2\text{mJ}^{-2}$ in agreement to that reported for YbCuAl [28]. Another interesting relation in *Heavy Fermion* systems is the *Wilson ratio* when compared the low temperature susceptibility $\chi(0)$ and the γ values. A linear correlation between these parameters is obtained for several concentrations of the $Yb_{1-x}Y_xCuAl$ series, as shown in Fig. 8(b), which indicates that the ratio $\chi(0)/\gamma$ is essentially constant, in agreement to that reported for YbCuAl [29].

As commented above, following the relations $\gamma \sim 1/T_K$ and $T_{max} \propto T_K$ [2,23], it is expected an increase of T_K with the Y dilution process. This

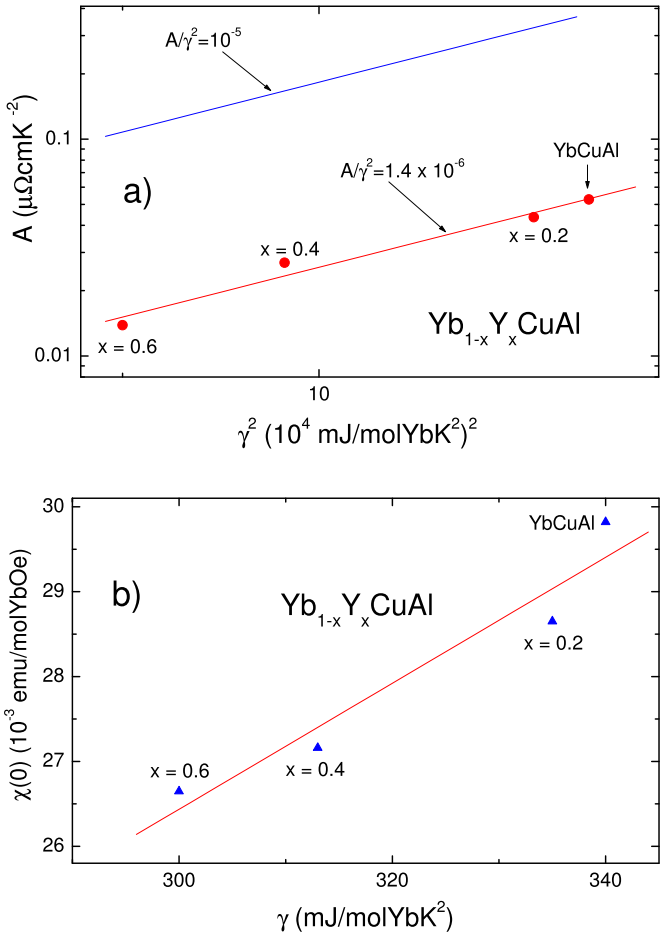

Fig. 8. a) Relation of A coefficient of the Fermi liquid dependence of the electrical resistivity at low temperatures (Table 1) with the γ^2 values for high Yb concentrations of $Yb_{1-x}Y_xCuAl$ series of alloys in log-log scale. A deviation from the value of $A/\gamma^2 = 1{\cdot}10^{-5}$ of heavy fermion systems is observed. b) Low temperature magnetic susceptibility ($\chi(0)$) in the Pauli regime vs. the electronic coefficient (γ), showing a constant Wilson ratio ($\chi(0)/\gamma$) along the $Yb_{1-x}Y_xCuAl$ series of alloys.

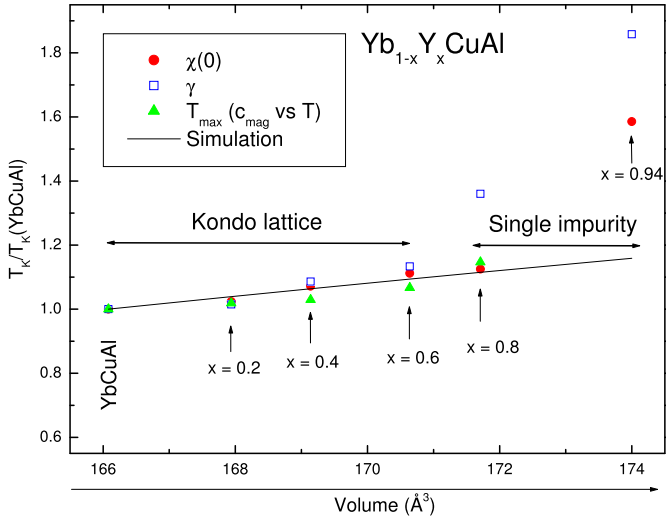

Fig. 9. Estimate of the Kondo temperature (T_K) values as function of the unit cell volume obtained from the relations: $\chi(0) \sim \gamma \sim T_K^{-1}$, and $T_K \sim T_{max}$ from the dc magnetic susceptibility and specific heat results. The solid line is a simulation with $T_K \propto exp(-1/Jn_f)$, according to the Jn_f unit cell volume dependence [30].

finding is supported by the observed decreasing values of low temperature susceptibility $\chi(0)$, by measurements of the magnetic properties ($\chi(0) \propto 1/T_K$) [2,23]. Thus, it is possible to estimate the variation of T_K respect to the reference YbCuAl alloy with the Y dilution, or with the change of the unit cell volume (see inset of Fig. 1), according to the behavior of the above parameters, and the result is depicted in Fig. 9. The values obtained for γ in $x = 0.8$ and 0.94, and also $\chi(0)$ for the last alloy (see inset of Fig. 7) give an overestimate of the T_K, not following the general tendency of the rest of samples. It is worth noticing, that for these concentrations we have observed a change from *Kondo lattice* ($x < 0.8$) to single impurity behavior. Thus, a regular behavior in the estimated T_K values is observed for samples showing a Kondo lattice behavior. Since $T_K \propto exp(-1/Jn_f)$, the variation of T_K is also in intimate relation with changes in the Jn_f product. Moreover, within the model of a compressible *Kondo lattice* the variation of Jn_f with the unit cell volume for the series of alloy is given by [30]:

$$|Jn_f|_x = |Jn_f|_0 exp[-q(V_x - V_0)]/V_0 \quad (1)$$

Where q is a parameter and $|Jn_f|_0$ and V_0 are the values for the reference YbCuAl ($x = 0$) alloy. Then, T_K is also a function of the unit cell volume as:

$$\frac{T_K(x)}{T_K(YbCuAL)} = exp\{1 - exp[q(V_x - V_0)/V_0]/|Jn_f|_0\} \quad (2)$$

From Eq. (1) it is expected a rise in the $|Jn_f|$ parameter with the increase of the unit cell volume (or Y dilution) (when q is negative), and consequently an increase in T_K parameter, as observed from the analysis of experimental data. For Yb compounds the parameter q displays a negative value, in contrast with the case for Ce-based compounds in which q is positive and usually taken between 6 and 8 [31]. If we assume $q = -6$ for our case, and leave $|Jn_f|_0$ as a free parameter, the results of the simulation of T_K dependence with the unit cell volume are depicted by a solid line in Fig. 9. Here, a value of $|Jn_f|_0 = 1.7$ is obtained, which is higher to that obtained for $YbCu_5$ ($|Jn_f| = 0.2$) [31] and Ce_3Al ($|Jn_f| = 0.6$) [32].

5. Conclusions

The chemical substitution of Yb by Y in $Yb_{1-x}Y_xCuAl$ series of alloys allowed to study the *negative pressure effects* on the pristine YbCuAl alloy with the increase of the unit cell volume. This affects the Kondo and *Heavy Fermion* behavior along the series, for which an increase of T_K and a decrease of the γ values are observed. Thus, the system is moving away from the QPC to the right-hand side of the peak in Doniach's magnetic phase diagram [3–5], to higher hybridization states, losing progressively the *Heavy Fermion* properties and displaying the concomitant increase of T_K, in agreement with such a diagram. Further studies appear necessary in the region of higher Y concentration ($0.7 \leq x < 1$) where a deviation from a general tendency of T_K, and a change of regime from *Kondo lattice* to single impurity behavior is observed.

Acknowledgements

This work was supported by the Spanish MINECO under project MAT2014-55049-C2-R and FAPESP - Brazil. DPR also acknowledges the financial support from FAPESP - Brazil PhD programme (grant 1998/10011-8).

References

[1] P. Schlottmann, Handbook of Magnetic Materials, in: K. H. J. Buschow (Ed.) (North Holland, Amsterdam, 2014), 23, p. 85.
[2] A.C. Hewson, The Kondo Problem to Heavy Fermions, Cambridge University Press, England, 1997.
[3] P. Coleman, Heavy Fermions: Electrons at the Edge of Magnetism, Handbook of

Magnetism and Advanced Magnetic Materials (Chichester, Wiley, 2007).
[4] S. Doniach, Physica B 91 (1977) 231.
[5] S. Doniach, Valence Instability and Related Narow Band Phenomena, R.D. Parks (ed.) (New York, Plenum, 1977).
[6] J.R. Iglesias, C. Lacroix, B. Coqblin, Phys. Rev. B 56 (1997) 11820.
[7] D.P. Rojas, A.N. Medina, F.G. Gandra, L.P. Cardoso, Phys. Rev. B 63 (2001) 165114.
[8] W.C.M. Mattens, P.F. de Chatel, A.C. Moleman, F.R. de Boer, Physica B 96 B (1979) 138.
[9] W.C.M. Mattens, H. Holscher, G.J.M. Tuin, A.C. Moleman, F.R. de Boer, J. Magn. Magn. Mater. 15–18 (1980) 982.
[10] A. Bleckwedel, A. Eichler, R. Pott, Physica B 107 (1981) 93.
[11] R. Pott, R. Schefzyk, D. Wohlleben, A. Junod, Z. Phys. B 44 (1981) 17.
[12] W. C. M. Mattens, J. Aarts, A. C. Moleman, I. Rachman, F.R. de Boer, Proceedings International Conference on Valence Instabilities, Zurich, P. Wachter and H. Boppart, (eds.)(Amsterdam, North-Holland, 1982) p. 211.
[13] G. van Kalkeren, H. van Nassou, F.R. de Boer, J. Magn. Magn. Mater. 47 & 48 (1985) 105.
[14] K. Alami-Yadri, H. Wilhelm, D. Jaccard, Sol. State Commun. 108 (1998) 279.
[15] H. Yamaoka, N. Tsujii, Y. Utsumi, H. Sato, I. Jarrige, Y. Yamamoto, Jung-Fu Lin, N. Hiraoka, H. Ishii, Ku-Ding Tsuei, J. Mizuki, Phys. Rev. B 87 (2013) 205120.
[16] J.D. Thompson, J.M. Lawrence, Handbook on the Physics and Chemistry of Rare Earth, K.A. Gschneidner Jr, L. Eyring, G.H. Lander, G.R. Choppin (eds.) (Amsterdam, North-Holland, 1994), 19, 133, p. 383.
[17] D.P. Rojas, M.S. thesis, Campinas State University (1998). ⟨http://repositorio.unicamp.br/jspui/handle/REPOSIP/277761⟩.
[18] L.S. Azechi, R.F. da Costa, A.N. Medina, F.G. Gandra, Rev. Fis. Apl. Instrum. 10 (1995) 70.
[19] L.S. Azechi, A.N. Medina, F.G. Gandra, J. Appl. Phys. 81 (1997) 4179.
[20] J.C. Lashley, M.F. Hundley, A. Migliori, J.L. Sarrao, P.G. Pagliuso, T.W. Darling, M. Jaime, J.C. Cooley, W.L. Hults, L. Morales, D.J. Thoma, J.L. Smith, J. Boerio-Goates, B.F. Woodfield, G.R. Stewart, R.A. Fisher, N.E. Phillips, Cryogenics 43 (2003) 369.
[21] J. Ziman, Electrons and Phonons, W. Marshall and D. H. Wilkinson (eds.) (Oxford, Clarendon, 1960).
[22] E.S.R. Gopal, Specific Heat at Low Temperatures, Plenum Press, New York, 1966.
[23] V.T. Rajan, Phys. Rev. Lett. 51 (1983) 308.
[24] P.S. Riseborough, J.M. Lawrence, Rep. Prog. Phys. 79 (2016) 084501.
[25] A.C. Hewson, D.M. Newns, J.W. Rasul, N. Read, J. Magn. Magn. Mater. 47 & 48 (1985) 354.
[26] D.P. Rojas, L. Fernández Barquín, J.I. Espeso, J. Rodríguez Fernández, J. Chaboy, Phys. Rev. B 78 (2008) 094412.
[27] B.M. Stelmakhovych, Yu.B. Kuzma, V.S. Babizhetsky, J. Alloy. Compd. 190 (1993) 161.
[28] N. Tsujii, K. Yoshimura, K. Kosuge, J. Phys: Cond. Matter 15 (2003) 1993.
[29] P. Schlottmann, Phys. Reports 181 (1989) 11119.
[30] M. Lavagna, C. Lacroix, M. Cryot, J. Phys. F 13 (1983) 1007.
[31] N. Tsujii, K. Yoshimura, K. Kosugue, H. Michor, K. Kreiner, G. Hilscher, Phys. Rev. B 55 (1997) 1032.
[32] A.N. Medina, M.A. Hayashi, L.P. Cardoso, S. Gama, F.G. Gandra, Phys. Rev. B 57 (1998) 5900.